

**Magnetization studies and random-field effects in  $U_{1-x}Pu_xSb$  single crystals**D. Kolberg,<sup>1,2</sup> F. Wastin,<sup>1</sup> J. Rebizant,<sup>1</sup> G. H. Lander,<sup>1</sup> and J. Schoenes<sup>2</sup><sup>1</sup>European Commission, Joint Research Centre, Institute for Transuranium Elements, Postfach 2340, D-76125 Karlsruhe, Germany<sup>2</sup>Institut für Halbleiterphysik und Optik, Technische Universität Braunschweig, Mendelssohnstr. 3, D-38106 Braunschweig, Germany

(Received 7 June 2002; revised manuscript received 15 August 2002; published 31 October 2002)

Single crystals of three concentrations  $x$  of  $U_{1-x}Pu_xSb$  have been grown by the mineralization technique. They crystallize in the cubic sodium chloride structure. After encapsulation, magnetization and susceptibility measurements have been done in the three main crystallographic directions. Effective moments  $\mu_{eff}$  and Curie temperatures are calculated for the paramagnetic phase, as well as Néel temperatures for the transition to the magnetically ordered phase. For  $x=0.25$  and  $x=0.50$  the magnetic structure is the same as in  $USb$ . Special attention has been given to  $x=0.75$ . Two transitions are observed in these samples, one to a triple  $\vec{k}$  structure below 93 K and a second one to a region with mixed triple  $\vec{k}$  and single  $\vec{k}$  character below 55 K. Susceptibility curves in this low-temperature region are rather complicated, but may be understood by taking into account the random distribution of uranium and plutonium ions on the crystal lattice. The random-field model for two different kinds of magnetic ions can explain the unusual shape of susceptibility curves for  $U_{1-x}Pu_xSb$ .

DOI: 10.1103/PhysRevB.66.134433

PACS number(s): 75.30.Kz, 75.50.Ee, 75.60.Ch

**I. INTRODUCTION**

Two of the most prominent actinide compounds are  $USb$  and  $PuSb$  because of their unusual magnetic properties. A considerable effort has been made by experimentalists as well as theorists (for the experiments see Refs. 1–3, for the theory Refs. 4–7) to understand the mechanisms which give rise to the complicated magnetic structures of  $PuSb$  and  $USb$ .

So far many magnetization studies have been undertaken on actinide mononictide and monochalcogenide solid solutions which all crystallize in the simple sodium chloride structure. Roughly they can be grouped into three types.

(1) The magnetic  $5f$  ion (in most cases uranium) forms a compound with pnictide and chalcogenide ions standing in the same *row* of the periodic table, such as, for instance,  $USb_xTe_{1-x}$ . Due to the chalcogen, an additional conduction electron with nominally  $d$  character is introduced, which hybridizes with the actinide  $5f$  electrons. The transition from one magnetic structure to another one is due to increasing hybridization of the conduction electrons with actinide  $5f$  or  $d$  electrons.

(2) In this case the solid solution is formed with ligands chosen from the same *column* of the periodic table, i.e.,  $US_xSe_{1-x}$ . This results mainly in an increasing lattice parameter in going down a chosen column and corresponds to an increase of the localization of the actinide ion.

(3) The easiest way to change the magnetic interactions by alloying is to use a nonmagnetic ion to form a diluted magnetic system, such as, for instance,  $Y_{1-x}Pu_xSb$ . This is a clean way to change the average distance between the magnetic ions, thereby lowering the magnetic interactions between them, and the valency of the diluents is usually known. Yttrium and lanthanum are known to be trivalent, whereas thorium acts like a tetravalent diluent.

It is clear that in the present study there is a qualitative difference to all magnetization studies done so far since the chosen solid solution  $U_{1-x}Pu_xSb$  does not fit in the scheme given above. It is the first magnetization study on actinide

$NaCl$  compounds in which two different magnetic ions are present in the same crystallographic matrix.

Rebizant *et al.*<sup>8</sup> have grown single crystals of the solid solution  $U_{1-x}Pu_xSb$  with  $x=0.25$ ,  $0.50$ , and  $0.75$  and characterized them. All samples crystallize in the  $NaCl$ -type structure. The first physical properties characterization was obtained by resistivity measurements on these compounds at the European Institute for Transuranium Elements.<sup>8</sup>

**II. GROWTH OF SINGLE CRYSTALS AND PREPARATION FOR SUSCEPTIBILITY MEASUREMENTS**

The starting material  $PuSb$  was single crystalline and has been prepared by the mineralization technique.<sup>9,10</sup> Polycrystalline  $USb$  was obtained by solid-vapor reaction. Stoichiometric amounts of pelletized powder were encapsulated in a tungsten crucible, melted by an electron beam technique, and annealed for several days at temperatures just below the melting point. The temperature was then decreased to 1000 °C in a stepwise fashion. The remaining drop down to ambient temperature followed the thermal inertia of the furnace. Large single crystals of  $U_{1-x}Pu_xSb$  have been obtained and could be cleaved into pieces of typically  $2 \times 2 \times 2$  mm<sup>3</sup> for magnetization measurements.

The samples investigated here were mounted in sample holders consisting of Plexiglas rods with a hole. The contribution of these sample holders to the net measured signal can reach up to about 10% of the sample's signal itself. Furthermore, the sample holder signal is of combined magnetic and geometric origin. It results in a rather complicated shape of the Plexiglas contribution curves as a function of both temperature and applied field. Therefore, each empty container was measured separately before inserting the sample in order to subtract its contribution from the full measured magnetization. The Plexiglas rods used for  $U_{1-x}Pu_xSb$  have been treated mechanically to have a shape which allows orientation along the main crystallographic directions of the  $NaCl$  structure. Samples are fixed with a small amount of adhesive; one example is shown in Fig. 1. The encapsulation is

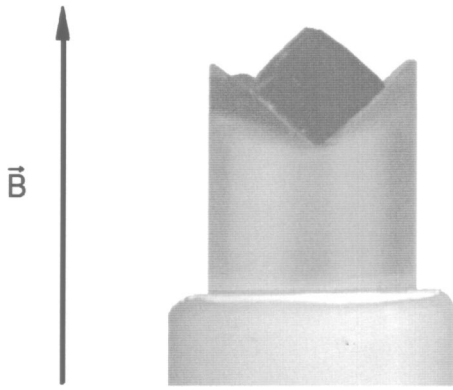


FIG. 1. Detail of sample holder including a 110-oriented  $U_{1-x}Pu_xSb$  single crystal. The outer diameter of the rod is  $\approx 6$  mm.

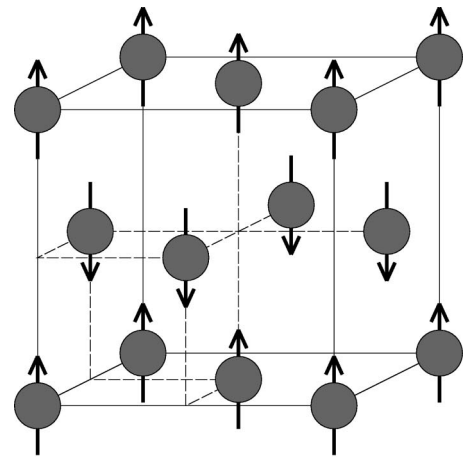
done with a tube made from new silver alloy (giving no contribution to the detected signal) sealed with *Stycast* with screws at top and bottom.

### III. PARENT COMPOUNDS

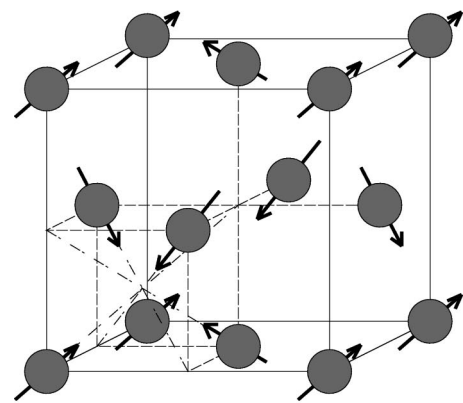
Since USb can be handled easily, the accumulated knowledge is much larger than that for PuSb. Uranium antimonide orders in a triple  $\vec{k}$  antiferromagnetic structure below the Néel temperature  $T_N=213$  K. The moments within each magnetic domain are oriented in the directions  $\langle 111 \rangle$ .<sup>11</sup> This arrangement is shown in Fig. 2 together with the single- $\vec{k}$  structure. The difference between these two structures can only be resolved experimentally by applying an external perturbation such as external pressures or magnetic fields. The ordered magnetic moment as derived from neutron experiments amounts to  $2.85\mu_B$ .<sup>12</sup> The electrical resistivity of USb shows a large upturn just below the Néel temperature,<sup>13</sup> which is now thought to be characteristic of the triple- $\vec{k}$  magnetic structure. The complicated Brillouin zone in paramagnetic phase is folded and becomes a simple cube having a volume only 1/4 of the original volume. Thus the number of free carriers becomes rather small in the ordered region. This is also supported by the electronic specific heat coefficient, which is roughly one order of magnitude smaller compared to other uranium pnictides.<sup>14</sup>

The susceptibility has been studied by Vogt *et al.*<sup>1</sup> and analyzed using a modified Curie-Weiss law. They found an effective moment of  $\mu_{eff}=3.64\mu_B$  per uranium ion and an additional contribution of conduction electrons with spins polarized antiparallel to the localized spins at the uranium sites.

The magnetic order which evolves in PuSb below 85 K is rather unusual; the magnetic phase diagram is displayed in Fig. 3. It becomes antiferromagnetic with an incommensurate magnetic structure. A commensurate structure with a wave vector  $\vec{k}=1/8$  is observed only in a small region of temperatures and magnetic fields. A further decrease of temperature results in a second transition to a ferromagnetic phase at approximately 68 K.<sup>15</sup> Again strong anisotropy has been found but with the magnetic moments directed along the  $\langle 100 \rangle$  direction.<sup>16</sup> The low-temperature magnetic mo-



(a)



(b)

FIG. 2. (a) Single  $\vec{k}$  and (b) triple  $\vec{k}$  (USb) type-I magnetic structures (Ref. 11).

ment of the plutonium ions is  $0.75\mu_B$  according to neutron studies.<sup>17</sup> This value is slightly smaller ( $0.64\mu_B$ ) in magnetization experiments due to conduction electron spins being aligned antiparallel to the Pu 5f moments.<sup>17</sup>

As in the case of USb an analysis of the high-temperature susceptibility in terms of a modified Curie-Weiss law yields

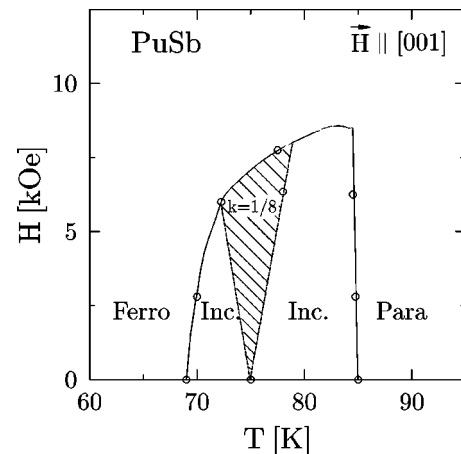


FIG. 3. Magnetic phase diagram of PuSb (Ref. 15).

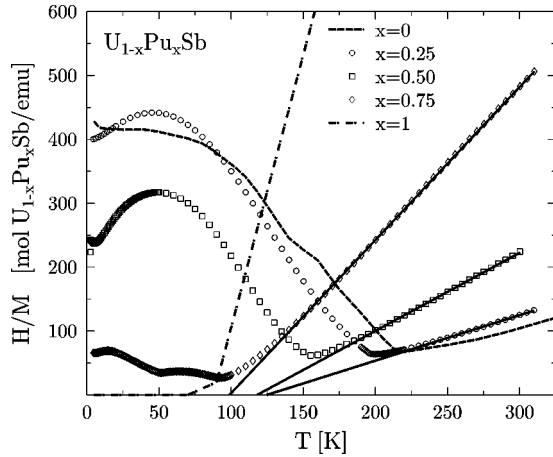


FIG. 4.  $H/M$  for  $U_{1-x}Pu_xSb$  in an external field of 10 kOe.

a contribution of conduction carriers  $\chi_0$  and one calculates an effective moment of  $\mu_{eff} = 1.0\mu_B$  per Pu ion<sup>18</sup> in accordance with the theoretical assumption of a  $5f^5$  ground state in an intermediate-coupling scheme.

#### IV. PARAMAGNETIC STATE AND THE TRANSITION TO THE $3\vec{k}$ -ORDERED PHASE

A summary of the results on the solid solution with  $x=0.25, 0.50,$  and  $0.75$  is displayed in Fig. 4, which shows the applied magnetic field divided by the measured magnetization as a function of temperature. For comparison data for USb (Ref. 1) and PuSb (Ref. 18) are included as dashed and dash-dotted lines, respectively. The minima in these curves define the ordering temperatures  $T_N$ .

For temperatures higher than  $T_N$  the data can be expressed by a Curie-Weiss law. These fits are represented by the solid lines in Fig. 4. The intersections of the lines with the  $T$  axis give  $\Theta_P$ . The complete set of variables resulting from this type of fits is summarized in Fig. 5.

For concentrations  $x=0.25$  and  $0.50$  the curves show an upturn below the corresponding Néel temperatures similar to the case of USb, suggesting that the antiferromagnetic  $3\vec{k}$ -type structure is present for these concentrations.

Besides the expected susceptibility peak at  $T_N$  an increase of  $M/H$  is observed below about 50 K for  $x=0.25$  and  $0.50$ . This might be interpreted as the presence of a second magnetic phase which occurs at temperatures  $\leq 50$  K. However, combined neutron and x-ray magnetic scattering studies did not indicate a second phase transition for temperatures down to  $\approx 10$  K for all  $x$ .<sup>19</sup>

Figure 6 shows  $H/M$  in the low-temperature region for  $x=0.25$  and  $x=0.50$  in more detail. An explanation for the broad maximum centered at 50 K for both compounds with low plutonium content can be that the Pu ions partly act as paramagnetic diluents. A superposition of an antiferromagnetic contribution like in USb and a paramagnetic part due to plutonium ions should in principle account for this situation. Using free ion  $Pu^{3+}$  wave functions,<sup>20</sup> a constant susceptibility for USb (which is valid only below 50 K), and the nominal actinide concentrations one calculates a temperature

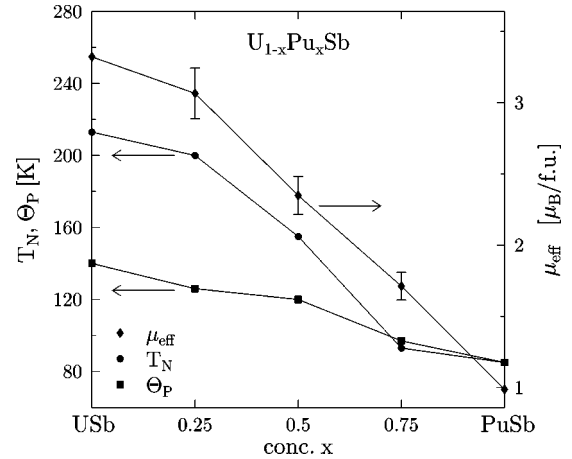


FIG. 5. Parameters calculated from Curie-Weiss fits as a function of the plutonium concentration; values of  $\mu_{eff}$  and  $\Theta_P$  for PuSb are taken from Ref. 18, and values of the Néel temperature are also included.  $T_N$  is shown without error bars since it is defined as the maximum in the  $\chi$  vs  $T$  curves. The uncertainty in this position is smaller than the symbol size used here. Error bars for the effective moments are presented in the figure. Compared to the uncertainty in  $\mu_{eff}$  errors in  $\Theta_P$  can be neglected.

dependence as shown by the dashed and dash-dotted lines in Fig. 6, and this clearly fails to explain the measurements. A much better description can be given by strongly reducing the paramagnetic contribution. The best fits are given by thick solid lines in Fig. 6. From these fits one concludes that only 10% of the plutonium ions in  $U_{0.75}Pu_{0.25}Sb$  and 25% of the plutonium ions in  $U_{0.50}Pu_{0.50}Sb$  form paramagnetic moments. However, the susceptibility of a magnetic free ion tends to infinity in the limit  $T \rightarrow 0$ . The departure of the susceptibility from the solid lines below  $T \approx 15$  K and the tendency to a fixed value shows up the twinlike nature of the plutonium ions in these solid solutions: at the same time they (i) give a minor paramagnetic contribution to the resulting susceptibility and (ii) take part in the magnetic order. Driven by uranium ions *the whole crystal* orders in the triple- $\vec{k}$  magnetic structure known from USb.

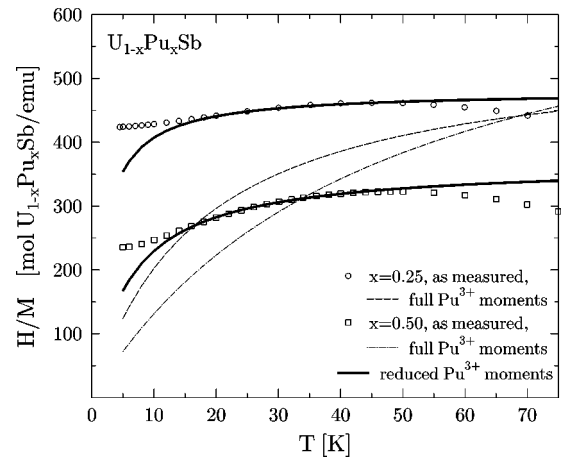


FIG. 6.  $H/M$  in the AF region for small Pu concentrations; for details, see text.

The Néel temperatures of USb and PuSb are 213 K and 85 K, respectively. Taking these values as measures for the exchange interaction, it becomes clear that the stability range for the  $3\vec{k}$  structure stemming from USb is larger than the one for the magnetic structures from PuSb. Hence, in the case of  $U_{0.50}Pu_{0.50}Sb$ , when the average U-U bond distance and the average Pu-Pu bond distance are equal, the magnetic structure is  $3\vec{k}$ .

It is known that the magnetic interactions in USb and other compounds are very long ranged. Theoretical investigations<sup>6</sup> on this subject point out that it is necessary to include more than the nearest-neighbor shell to describe the magnetism in this and similar compounds sufficiently well.<sup>21</sup>

The measurements have been done in the three main crystallographic directions of the sodium chloride structure. In the magnetically ordered phase one might ask for the easy magnetic axis of  $U_{1-x}Pu_xSb$ . However, the saturation fields for these samples are much higher than the external fields available with our superconducting quantum interference device (SQUID) magnetometer (70 kOe). Therefore, magnetization curves as a function of the applied field are essentially linear and independent of the crystal orientation with respect to the direction of the external field.

#### V. MAGNETIC PHASE DIAGRAM FOR $x=0.75$ AND RANDOM-FIELD EFFECTS

One might anticipate that further increasing the Pu content beyond  $x=0.50$  would lead to a behavior reminiscent of that of PuSb. Indeed, the shape of the curve for  $x=0.75$  in Fig. 4 changes dramatically and shows two prominent transitions as is the case in plutonium antimonide. However, the detailed phase diagram of  $U_{0.25}Pu_{0.75}Sb$  has been investigated using neutron scattering techniques.<sup>19</sup> Unexpectedly, one observes no ferromagnetism and no incommensurate phase at all, but a phase with a  $4+4-$  magnetic structure that is  $3\vec{k}$  at high temperature and undergoes a gradual transition to a  $1\vec{k}$  phase below  $\approx 55$  K. The wave vector does not change.

Since neutrons probe the magnetic moment at a given lattice site, whereas a magnetization study using a SQUID measures the net magnetic moment of a sample, a magnetic phase diagram drawn from magnetization studies can show more transition lines due to additional effects—for example, domain behavior—which are not related to microscopic phase transitions. Typical magnetization data are shown in Fig. 7 (ZFC refers to zero field cooling, FC to field cooling) together with a “phase diagram” derived from the present work in Fig. 8.

The borderline between paramagnetism and the two antiferromagnetic (AF) phases is detected via a peak in the second derivative of the magnetization with respect to temperature. This is shown by the vertical solid line in Fig. 8. The transition from the antiferromagnetic phase  $3\vec{k}$  to the single- $\vec{k}$  phase (dashed line in Fig. 8) present for temperatures between 55 K and 93 K is rather sluggish. A superposition of two Brillouin functions standing for the two phases results in a peak in the first derivative of the magnetization with re-

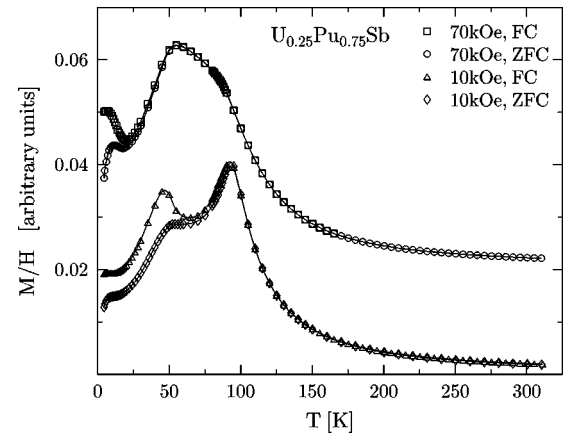


FIG. 7. Typical magnetization curves for  $U_{0.25}Pu_{0.75}Sb$ ; for clarity, curves for different fields have been shifted.

spect to the applied field. This peak is taken as the definition of the transition field and two examples for  $U_{0.25}Pu_{0.75}Sb$  are plotted in Fig. 9. This suggests some instability in the  $3\vec{k}$  structure, although it has not been observed with scattering techniques.

We propose that the remaining three dash-dotted lines in Fig. 8, which are not present in the phase diagram drawn from the neutron study, are a consequence of the random distribution of two types of magnetic ions in the investigated solid solution. The randomness of the positions of ions of a given type gives rise to the so-called random-field effects which have been studied in detail in transition element compounds such as, for instance,  $Fe_xZn_{1-x}F_2$ ,<sup>22</sup>  $Fe_xCo_{1-x}Cl_2$ ,<sup>23</sup> and by theory.<sup>24</sup> The starting point of the theoretical investigations was a crystal lattice with vacant sites as depicted in Fig. 10(a), whereas the analog in magnetism can appear in a perfect crystal lattice with *magnetically vacant* sites as shown in Fig. 10(b). In this case only one type of magnetic ion is present, and the random environment of a magnetic ion gives rise to different exchange interactions in different directions. However, the present system is best described as in

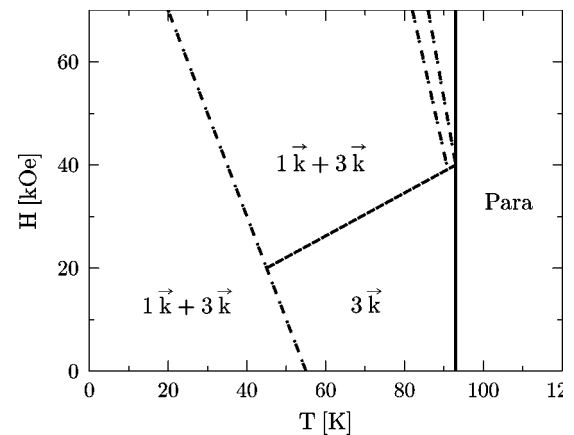


FIG. 8. Construction of phase diagram for  $U_{0.25}Pu_{0.75}Sb$  from combined magnetization and neutron studies. The transition lines are taken from magnetization anomalies; the assignment of structures is due to neutron experiments.



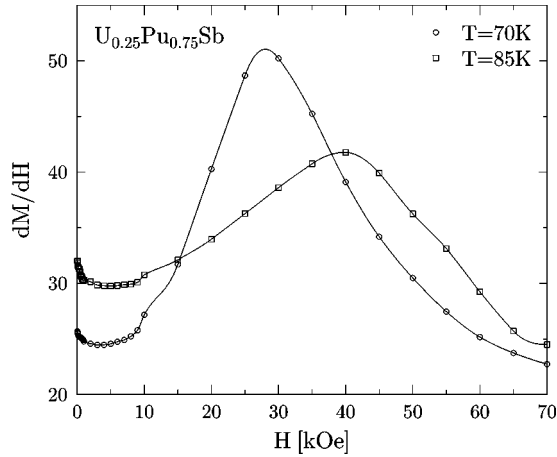


FIG. 9. First derivative of the magnetization with respect to the applied field, showing the field-dependent transition between the  $3\vec{k}$  and the single- $\vec{k}$  structures.

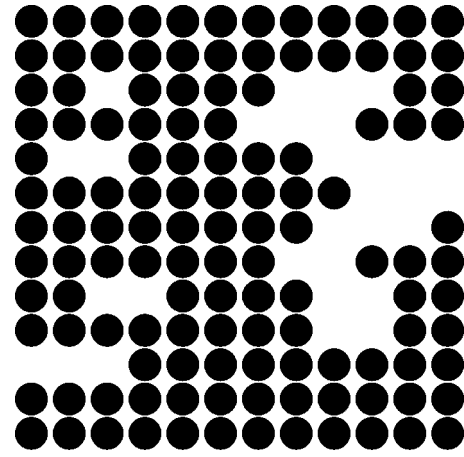
Fig. 10(c). All ions displayed are magnetic, but the size of the magnetic moment is different for the two types. Therefore the exchange is still random, but the strength of the induced effects depends on the difference of the magnetic moments of both types. The ordered moments have been measured to be  $2.85\mu_B$  and  $0.74\mu_B$  in USb and PuSb, respectively.<sup>25</sup> Hence, the difference in the uranium and plutonium moments is expected to be quite substantial by  $\approx 2.1\mu_B$ . In a magnetization experiment this leads to a strong field dependence of random-field effects. Moreover, the Pu-Pu exchange tends to favor a  $\langle 100 \rangle$  moment alignment, whereas the U-U exchange favors a  $\langle 111 \rangle$  alignment. An important additional point, shown by the x-ray studies, is that the magnetic ordering in this material is never long range, but consists of correlations of  $\approx 400 \text{ \AA}$ .

The diluted antiferromagnet in a field (DAFF) has been investigated in Ref. 26. Using a Hamiltonian for the Ising model and an additional term which serves to create a random field,

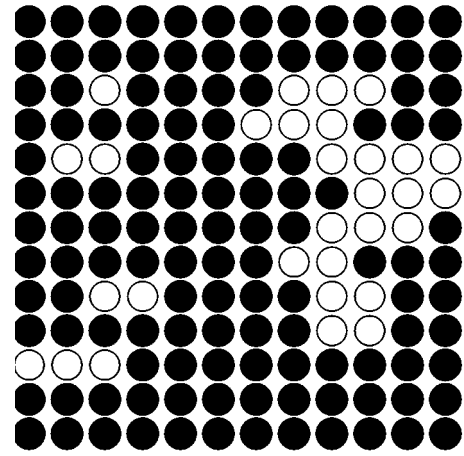
$$H = - \sum_{i,j} J_{ij} S_i^z S_j^z - \sum_i (h + h_i) S_i, \quad (1)$$

where  $h$  is the externally applied field, and  $h_i$  the random exchange field acting on spin  $S_i$ , the authors calculated magnetizations and specific heats as a function of temperature and applied magnetic field. Calculations were done in mean-field approximation as well as in Monte Carlo simulations. The results are qualitatively similar and the Monte Carlo result is depicted in Fig. 11 (upper panel), together with magnetization measurements on  $U_{0.25}Pu_{0.75}Sb$  (lower panel). The theory was developed for a direct transition from the paramagnetic to a magnetically ordered state. Therefore the appearance of the  $3\vec{k}$  structure in low fields (and above  $T = 55 \text{ K}$ ) complicates a direct comparison, but one finds a remarkable agreement between our experiments and theory.

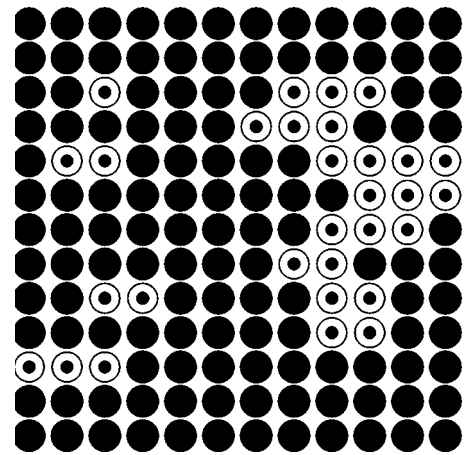
Cooling the sample in zero field allows a random development of the domains; however, when a field is applied the antiferromagnetic domains show unusual behavior, which gives rise to jumps in the magnetization, as shown in Fig. 12.



(a)



(b)



(c)

FIG. 10. (a) “Random bonds.” (b) Random exchange, e.g.,  $La_{1-x}U_xS$  (sulfur ions are not displayed since their distribution is regular). Black, magnetic; white, nonmagnetic. (c) The case of  $U_{1-x}Pu_xSb$ . Black, magnetic; dotted, less magnetic.

We speculate that the domains develop over a longer range when the field is applied, and the subsequent realignment of them parallel to the field costs more energy. It is important to stress that in the high-temperature stable  $3\vec{k}$  phase there are no domains, so this behavior is not expected.

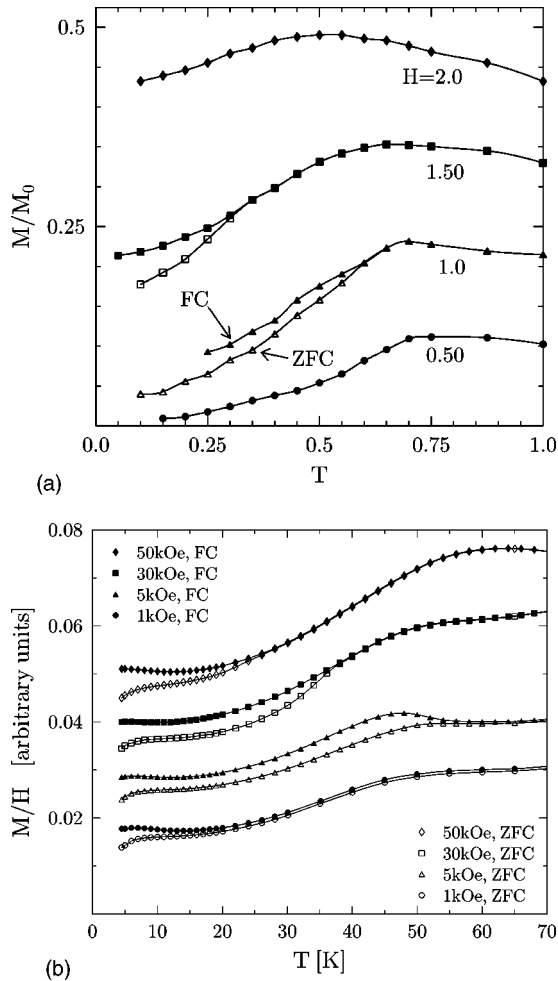


FIG. 11. Monte Carlo simulations (upper panel), results for  $U_{0.25}Pu_{0.75}Sb$  (lower panel); symbols are chosen so as to provide direct comparison to the theory.

The observed jumps in the magnetization are only visible when the sample is cooled in an applied magnetic field, which gives strong support for the above-mentioned explanation of the magnetization behavior in terms of random-field effects. For comparison, a measurement with the sample cooled in zero field is included in Fig. 12. In addition, in the inset the high-field part of a hysteresis loop is shown for  $T = 87.5$  K. At this temperature one can follow both jumps and their hysteretic properties, which are typical for the behavior of domain walls. One can now analyze the positions of jumps as a function of the applied magnetic field. This is shown in Fig. 13 which corresponds to the upper right quarter of the phase diagram presented in Fig. 8. It should be emphasized that these effects occur exclusively in the single- $\vec{k}$  structure because of the presence of domains.

Interestingly, the compound  $U_{0.50}Pu_{0.50}Sb$  shows similar behavior in very low fields (as well as in zero field, as pointed out in Ref. 8): there is a difference in zero-field-cooled magnetization data compared to the field cooled curves below 55 K, as depicted in Fig. 14.

It should be emphasized that the occurrence of random-field effects requires the coexistence of two types of mag-

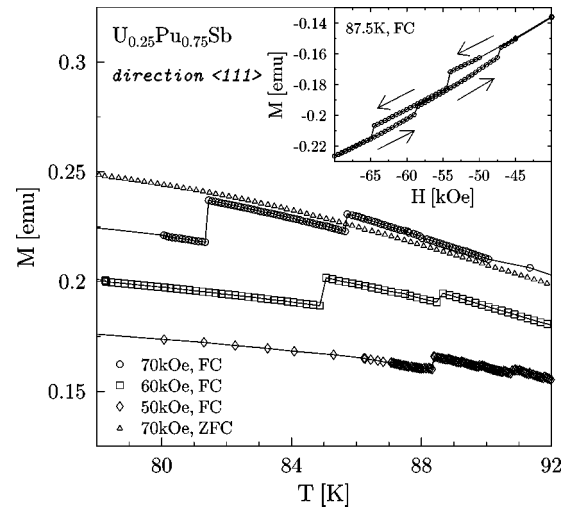


FIG. 12. Magnetization jumps in  $U_{0.25}Pu_{0.75}Sb$  due to domain wall motion (FC curves). For comparison, one of our ZFC measurements has been included. The inset shows data as a function of the applied field to demonstrate the hysteretic behavior of both jumps.

netic ions: type A carrying a particular magnetic moment different from the moment at lattice sites of type B. Therefore, in a first approximation one may treat the uranium and plutonium ions independently. Accordingly, one can try to describe the magnetic properties of  $U_{1-x}Pu_xSb$  in terms of more general physics, neglecting effects typically found in  $5f$ -electron magnetism.

To find the reason for the rather unexpected appearance of the  $1\vec{k}$  phase it is useful to draw the lattice parameters of the solid solution  $U_{1-x}Pu_xSb$ .<sup>8</sup> Figure 15 shows that the single- $\vec{k}$  structure is associated with an increasing lattice parameter which in the case of  $U_{0.25}Pu_{0.75}Sb$  is reminiscent of a fictitious  $(Np,Pu)Sb$  solid solution and might be compared with pure  $NpSb$  under pressure. Clearly, the  $3\vec{k}$  structure of  $U_{0.25}Pu_{0.75}Sb$  is stabilized since the magnetic order of  $NpSb$  is of the same type (despite a different wave vector). More-

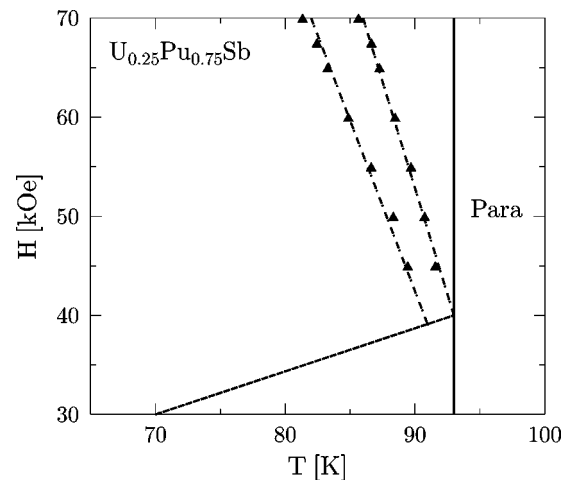


FIG. 13. Detail of the magnetic phase diagram of  $U_{0.25}Pu_{0.75}Sb$  (see Fig. 8); shown with solid triangles are the experimentally observed positions of sudden domain wall motions in the  $H$ - $T$  plane.

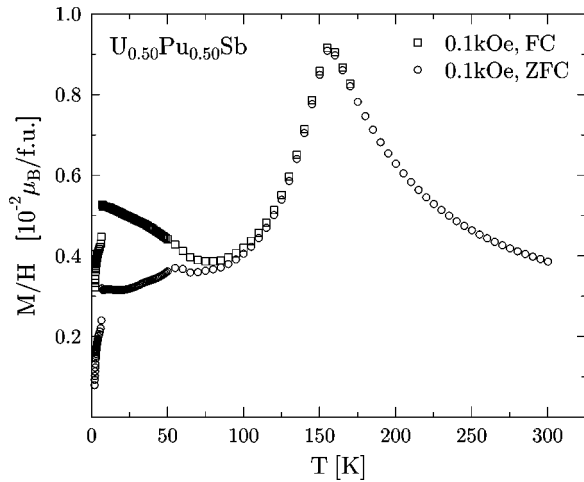


FIG. 14.  $M/H$  for  $U_{0.50}Pu_{0.50}Sb$  in low fields.

over, high-pressure resistivity studies on  $NpSb$  (Ref. 27) showed a magnetic phase transition and it was suggested that the pressure-induced magnetic phase is of single- $\vec{k}$  type.

On the other hand, one can decrease the lattice parameter in going up in the pnictogen column of the periodic table starting from  $NpSb$ . The same effect appears again: in addition to the  $3\vec{k}$  structure typical for neptunium pnictides single- $\vec{k}$  phases are observed in  $NpAs$  and  $NpP$ .

The possible influence of the lattice parameter can also be seen without referring to neptunium compounds. The plutonium pnictides with small lattice constants order ferromagnetically. Staying in this column of the periodic table one observes a trend to establish antiferromagnetic structures with increasing Pu-Pu distance,  $PuSb$  being in a critical position. This transition is completed for  $PuBi$  which orders in a single- $\vec{k}$  AF structure and does not show a further transition to ferromagnetism. Therefore, if one imagines  $U_{0.25}Pu_{0.75}Sb$  as plutonium antimonide with too large a lattice parameter, one would anticipate an enlarged stability range for  $1\vec{k}$  antiferromagnetic structures.

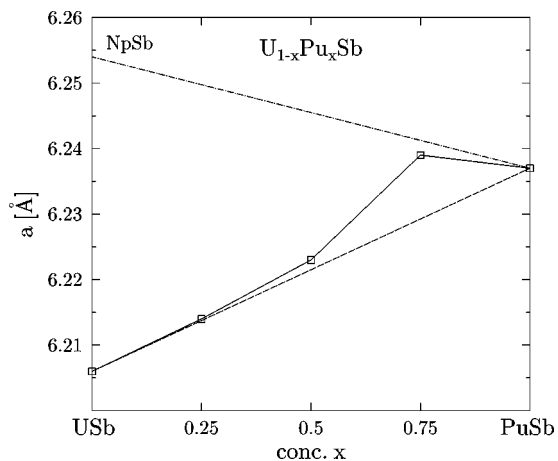


FIG. 15. Lattice parameter as a function of plutonium concentration.

## VI. SUMMARY

In all studies done so far on actinide NaCl structured binary and pseudobinary compounds it was chosen to either change the concentration of anions [e.g.,  $USb_xTe_{1-x}$  (Ref. 11)] or to dilute the magnetic actinide ions with nonmagnetic Y, La, or Th [as in  $Pu_xY_{1-x}Sb$  (Ref. 1) or in  $U_xY_{1-x}Sb$  (Ref. 28)]. In the present work a qualitatively new type of single-crystalline sample has been investigated:  $U_{1-x}Pu_xSb$  is the first series of NaCl-structured pseudobinary compounds that contains two types of magnetic actinide constituents, uranium and plutonium.

Substituting uranium with plutonium results in a decrease of the ordering temperature from its value for  $USb$  (213 K) down to  $T_N=155$  K for  $U_{0.50}Pu_{0.50}Sb$ . The average effective magnetic moments and paramagnetic Curie temperatures have been calculated from a simple Curie-Weiss law. Hence, in the paramagnetic temperature range no crystal field transitions or additional contributions due to conduction electrons are observed.  $\mu_{eff}$  and  $\Theta_P$  decrease as expected from the comparison with parameters for the end compounds. The triple- $\vec{k}$  magnetic structure characteristic for  $USb$  stays stable in this concentration range.

The case of  $U_{0.25}Pu_{0.75}Sb$  deserves special attention. For this high Pu concentration one would anticipate the occurrence of a ferromagnetic phase since this is found in pure  $PuSb$ . In contrast to the expected ferromagnetism in the  $x=0.75$  sample at low temperature, the composition changes from triple  $\vec{k}$  at high temperature to single  $\vec{k}$  at lower temperature below  $\approx 55$  K. The magnetic propagation in both phases is  $k=0.25$  rlu, so that the stacking sequence is  $4+$ ,  $4-$ . Above a field of roughly 35 kOe the  $1\vec{k}$  antiferromagnetic structure is stable for all  $T < T_N$ .<sup>19</sup> It is found also with the higher-temperature magnetic structure of pure  $PuSb$ . Although the physical origin for the stability of the  $1\vec{k}$  structure is not well understood, close inspection of the trends for the evolution of magnetism in actinide monpnictides led us to qualitative arguments for its appearance in  $U_{0.25}Pu_{0.75}Sb$ .

A striking feature of the phase diagram deduced from magnetization curves is the appearance of additional features for certain regions of temperatures and magnetic fields. These features occur exclusively in the single- $\vec{k}$  phase and are associated with domain behavior in the single- $\vec{k}$  phase. For instance, in the low-temperature range there is a difference between the ZFC and FC magnetization data. A model has been proposed which can explain these differences. It is based on the distribution of uranium and plutonium ions onto the available lattice sites. If two species of randomly distributed magnetic ions carry considerably different amounts of magnetic moments, then a random field stemming from its surrounding will act on each ion. The random-field model, originally developed for solid solutions containing transition metals, can explain our experimental findings for  $U_{0.25}Pu_{0.75}Sb$ .

## ACKNOWLEDGMENTS

D.K. acknowledges the European Commission for support in the frame of the program "Training and Mobility of Re-

searchers.” The high-purity Pu metal required for the fabrication of this compound was made available through a loan agreement between Lawrence Livermore National Labora-

tory and the European Institute for Transuranium Elements, in the frame of a collaboration involving LLNL, Los Alamos National Laboratory, and the U.S. Department of Energy.

- <sup>1</sup>O. Vogt and K. Mattenberger, in *Handbook on the Physics and Chemistry of the Rare Earths*, edited by K.A. Gschneidner, Jr., L. Eyring, G.H. Lander, and G. R. Choppin (Elsevier, Amsterdam, 1993), Vol. 17.
- <sup>2</sup>G.H. Lander and W.G. Stirling, *Phys. Rev. B* **21**, 436 (1980).
- <sup>3</sup>B. Hålg and A. Furrer, *Phys. Rev. B* **34**, 6258 (1986).
- <sup>4</sup>J. Jensen and P. Bak, *Phys. Rev. B* **23**, 6180 (1981).
- <sup>5</sup>G.-J. Hu and B.R. Cooper, *Phys. Rev. B* **48**, 12 743 (1993).
- <sup>6</sup>H. Yamagami, *Phys. Rev. B* **61**, 6246 (2000).
- <sup>7</sup>K. Knöpfle and L.M. Sandratskii, *Phys. Rev. B* **63**, 014411 (2000).
- <sup>8</sup>J. Rebizant, F. Wastin, C. Rijkeboer, E. Bednarczyk, and P. Lefèvre, *J. Alloys Compd.* **271-273**, 490 (1998).
- <sup>9</sup>J.-C. Spirlet, *J. Nucl. Mater.* **166**, 41 (1989).
- <sup>10</sup>J.-C. Spirlet and O. Vogt, in *Handbook on the Physics and Chemistry of the Actinides*, edited by A. J. Freeman and G. H. Lander (Elsevier, Amsterdam, 1984), Vol. 1.
- <sup>11</sup>P. Burllet, J. Rossat-Mignod, S. Quezel, O. Vogt, J.C. Spirlet, and J. Rebizant, *J. Less-Common Met.* **121**, 121 (1986).
- <sup>12</sup>G.H. Lander and P. Burllet, *Physica B* **215**, 7 (1995).
- <sup>13</sup>J. Schoenes, B. Frick, and O. Vogt, *Phys. Rev. B* **30**, 6578 (1984).
- <sup>14</sup>H. Rudigier, H.R. Ott, and O. Vogt, *Phys. Rev. B* **32**, 4584 (1985).
- <sup>15</sup>P. Burllet, S. Quezel, J. Rossat-Mignod, J.C. Spirlet, J. Rebizant, W. Müller, and O. Vogt, *Phys. Rev. B* **30**, 6660 (1984).
- <sup>16</sup>B.R. Cooper, P. Thayamballi, J.C. Spirlet, W. Müller, and O. Vogt, *Phys. Rev. Lett.* **51**, 2418 (1983).
- <sup>17</sup>G.H. Lander, A. Delapalme, P.J. Brown, J.C. Spirlet, J. Rebizant, and O. Vogt, *Phys. Rev. Lett.* **53**, 2262 (1984).
- <sup>18</sup>O. Vogt, K. Mattenberger, J. Löhle, and J. Rebizant, *J. Alloys Compd.* **271-273**, 508 (1998).
- <sup>19</sup>P.S. Normile, W.G. Stirling, D. Mannix, G.H. Lander, F. Wastin, J. Rebizant, F. Boudarot, P. Burllet, B. Lebech, and S. Coburn, *Phys. Rev. B* **66**, 014405 (2002); P.S. Normile, W.G. Stirling, D. Mannix, G.H. Lander, F. Wastin, J. Rebizant, and S. Coburn, *ibid.* **66**, 014406 (2002).
- <sup>20</sup>D.J. Lam and S.-K. Chan, *Phys. Rev. B* **6**, 307 (1972).
- <sup>21</sup>E.M. Collins, N. Kioussis, S.P. Lim, and B.R. Cooper, *J. Appl. Phys.* **85**, 6226 (1999).
- <sup>22</sup>D.P. Belanger, A.R. King, and V. Jaccarino, *Phys. Rev. B* **31**, 4538 (1985).
- <sup>23</sup>P. Wong, P.M. Horn, R.J. Birgeneau, and G. Shirane, *Phys. Rev. B* **27**, 428 (1983).
- <sup>24</sup>S. Fishman and A. Aharony, *J. Phys. C* **12**, L729 (1979).
- <sup>25</sup>G. H. Lander, in *Handbook on the Physics and Chemistry of the Rare Earths*, edited by K.A. Gschneidner, Jr., L. Eyring, G.H. Lander, and G.R. Choppin (Elsevier, Amsterdam, 1993), Vol. 17.
- <sup>26</sup>G.S. Grest, C.M. Soukoulis, and K. Levin, *Phys. Rev. Lett.* **56**, 1148 (1986); *Phys. Rev. B* **33**, 7659 (1986).
- <sup>27</sup>M. Amanowicz, D. Braithwaite, V. Ichas, U. Benedict, J. Rebizant, and J.C. Spirlet, *Phys. Rev. B* **50**, 6577 (1994).
- <sup>28</sup>B. Frick, J. Schoenes, F. Hulliger, and O. Vogt, *Solid State Commun.* **49**, 1133 (1984).